24th EUROPEAN ROTORCRAFT FORUM
Marseilles, France, 15th-17th September 1998

Session 'Structures and Materials' SM06

The Damage Tolerant Design of the EC135 Bearingless Main Rotor

H. Bansemir, K. Pfeifer
EUROCOPTER DEUTSCHLAND GmbH
81663 Munich, Germany

ECD-0087-98-PUB

The EC135 is a twin-engined multi-mission light helicopter of the new generation. The structure has been designed to meet the latest certification requirements including damage tolerance and crashworthiness according to JAR27. Fiber composite parts, however, have to meet the 'Special Condition' of the German airworthy authority Luftfahrtbundesamt (LBA) demanding damage tolerance behaviour and limit load capacity after fatigue testing.

One of the most significant features of the EC135 is its bearingless main rotor system (BMR). It is a consequent result of the ECD rotor development concerning simplification and reliability. Main emphasis was laid in an excellent fail safe behaviour of the fiber composite blades. The result is a life of more than 10 000 flight hours.

Special basic investigations were additionally performed to examine the fracture mechanical behaviour of the flexbeam with the help of finite element analysis and tests. The results can also help for other fiber composite structures in the determination of damage begin and damage growth.

After a short presentation of the EC135 design features, this paper describes the bearingless main rotor in detail including analysis, component tests and certification activities. Furthermore the investigations of the fracture mechanics are presented.

TABLE OF CONTENTS

Figure 1: The Multi-Mission Helicopter EC135

1. INTRODUCTION

Since the beginning of the sixties Eurocopter Germany, the former helicopter division of MBB, has been working in the field of fiber composites. The development of fiber composite rotor blades allowed the realization of new rotor concepts with remarkably increased life and reliability at reduced weight and maintenance costs.

In 1967 the MBB BO105 performed its maiden flight. The worldwide first serial hingeless main rotor system was a key element of this helicopter. The innovative rotor design included

new materials such as titanium for the rotor hub and fiber glass epoxy for the main and tail rotor blades. Due to the flexibility and high fatigue strength of the glass fiber composites, the flapping and lead-lag motions could be carried by bending of the blade root. Thus the corresponding hinges of a conventional rotor could be eliminated, but not the roller bearings, which were still necessary for the pitch motions of the blade. This new rotor system was a great progress with regard to weight and cost reduction due to the reduced number of parts and the high life and damage tolerant behaviour of the composite blades. Another benefit was the improved handling qualities and the excellent flight manoeuvrability especially in gusty weather conditions.

This twin light helicopter was the first to be certified according to the FAR27 regulations. Up to now almost 1500 BO105 multi-mission helicopters have been manufactured and are flying in more than 40 countries.

In 1983 the company started the development of an experimental twin helicopter designated BO108. Many technological advances were incorporated into the design. The first of two prototypes performed its maiden flight in October 1988. The innovative design included a bearingless (and also hingeless) main rotor system without bearings in main rotor blade functions. Lead-lag damping was provided by elastomeric dampers.

In close cooperation with the customers the design of the BO108 was revised. This led to the development of the multi-mission helicopter EC135 being started in 1991/92. The cabin was enlarged to take up to seven persons, and the maximum take-off weight was increased. The main rotor remained almost identical to that of the BO108, whereas the tailboom with the Fenestron anti-torque system was new developed by Eurocopter France.

Structural safety was one important requirement. Thus the design meets the latest certification requirements according to Joint Aviation Requirements JAR27 'Small Rotorcraft' and the 'Special Condition for Primary Structures Designed with Composite Material' of the German LBA. Fail safe design features were incorporated and damage tolerance evaluation was performed by analysis and by test.

The applied advanced technologies affect many systems and structural parts like modern avionics and the Anti Resonance Isolation System ARIS to achieve low vibration levels. Reduced noise as well as low maintenance costs are further exceptional features of the EC135. The noise signature is about 7 dB below the ICAO standard.

The first prototype carried out its first flight in February 1994, powered by two Turbomeca Arrius 2B engines, whereas the second prototype began its flight tests two months later, powered by the alternative Pratt & Whitney PW206B engines. After extensive testing of three prototypes, structures and systems and with the help of validated analysis, the type certificates were issued in June 1996 by the LBA and one month later by the French DGAC and the American FAA. Up to now more than 120 EC135 helicopters have been ordered by customers from all over the world.

Figure 2 shows a 3-view drawing and the overall dimensions of the C135, whereas Table 1 lists some main characteristics of the helicopter.

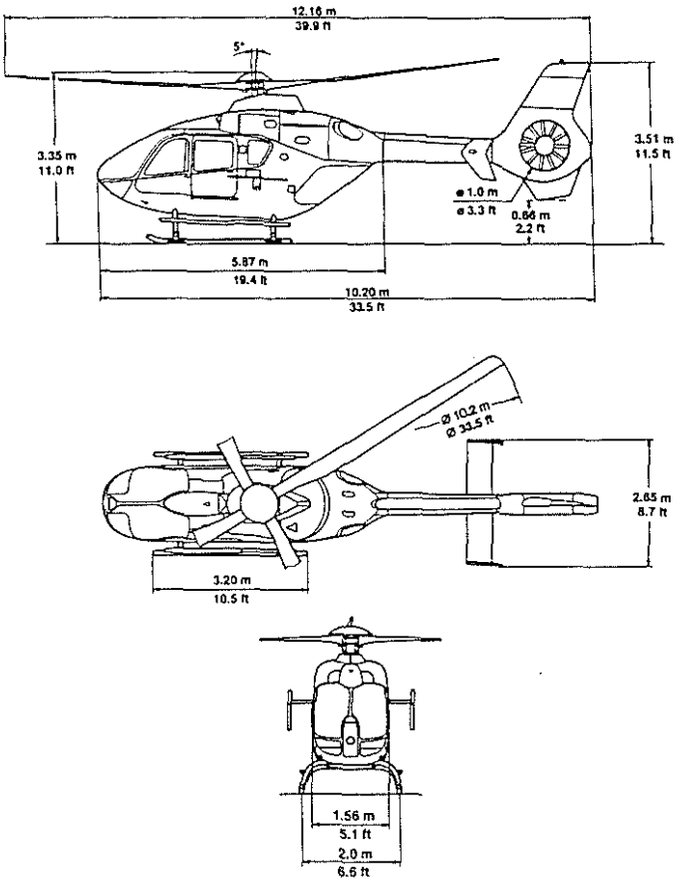

Figure 2: Three-View Drawing of the EC135

Table 1: Main Characteristics of the EC135 with Arrius 2B1 Engines

Empty Weight of Standard Aircraft	1465 kg	3230 lbs
Maximum Take-Off Weight	2720 kg	6000 ibs
MTOW with External Load	2900 kg	6393 lbs
Maximum Continuous Power	2 x 283 kW	
Take-Off Power	2 x 308 kW	
2.5 min OEI	1 x 411 kW	
Rotor RPM	100 - 104 %	
Blade Tip Speed	211 - 219 m/s	
Maximum Cruising Speed SL ISA	257 km/h	139 kts
Never Exceed Speed SL ISA	278 km/h	150 kts
Hover in Ground Effect	4040 m	13250 ft
Hover Out of Ground Effect	3100 m	10200 ft
Rate of Climb	8.4 m/s	1650 ft/min
Maximum Range	620 km	335 nm
Maximum Endurance	4:33 hrs	

2. DESCRIPTION OF THE BEARINGLESS MAIN ROTOR SYSTEM

One of the most significant features of the EC135 is the Bearingless Main Rotor (BMR) shown in Figure 3. It has a 50 kg weight reduction and 40% less parts compared to the BO105 rotor. The equivalent flapping hinge offset is about 9% of the blade radius. The rotor is a soft inplane design.

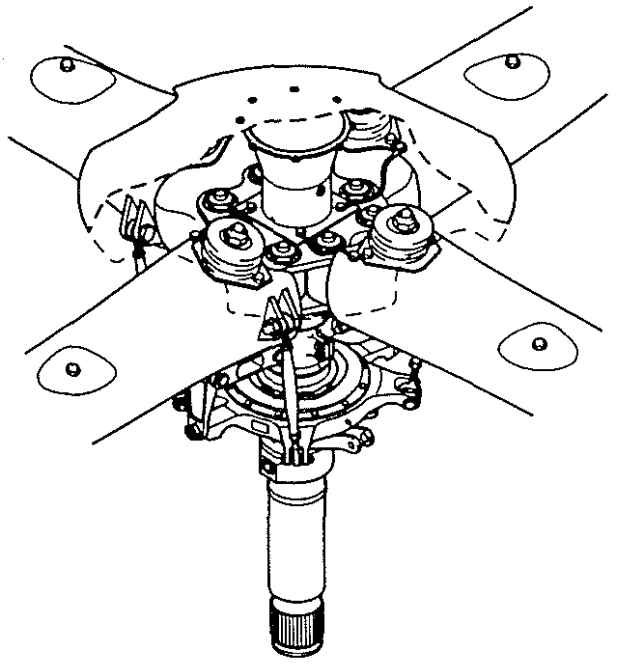

Figure 3: *The Inner Part of the EC135 Bearingless Main Rotor* System with Elastomeric Dampers

2.1 Rotor Hub and Shaft

The EC135 has a very simple rotor hub. In principle it consists of two plane plates connected with each other, between which the blades are bolted. Rotor hub and shaft are manufactured in one piece out of a forged steel blank (Fig. 4).

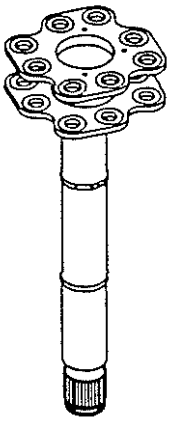

Figure 4: Rotor Hub and Shaft of the EC135

2.2 Main Rotor Blade

Whereas the rotor hub of the EC135 has an exceptionally simple design, the structure of the blade root has become rather complicated as it has to take on the tasks of the hinges and bearings of a conventional rotor. This blade root is also called flexbeam and is the key element of the bearingless rotor. A skilful design, however, allows the local separation of the different tasks in the flexbeam.

The blade and its inner part are shown in the Figures 5 and 6. It is a GFRP (glass fiber reinforced plastic) prepreg design using E-Glass and a 120°C epoxy system. It consists of unidirectional tapes orientated in the longitudinal direction. These are mainly *responsible for the longitudinal and bending stiffnesses and carry* the greatest part of the centrifugal force and the bending moments, whereas the ±45° layers in the shear web and the blade skin have to carry the greatest part of the shear loads including torsional moment.

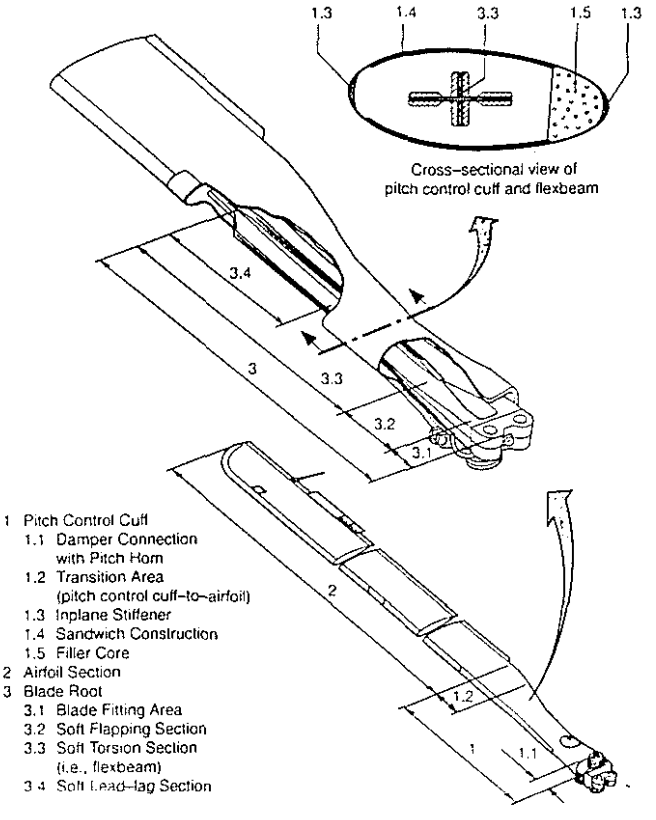

Figure 5: The Bearingless Main Rotor Blade

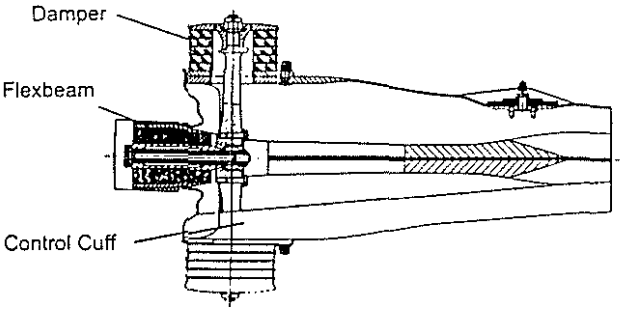

Figure 6: Blade Attachment Area with Control Cuff and Dampers

At radius station R = 110 mm the blade is connected with the help of two bolts to the rotor hub. The loads are transferred via two double lugs (Fig. 23) at the relatively stiff blade attachment area. A tapered transition area leads to the flat 'flapping hinge' section. This section has to allow the flap angles by bending.

In the following transition area the layers are shifted to the cruciform shape of the torsional element. This has a short length of about 0.5 m and replaces the blade bearings. Its slim and deeply slit cruciform cross section results in an extremely low torsional stiffness of the flexbeam of 4.2 Nm/° without and of 7.2 Nm/° with centrifugal force.

The cruciform shape of the torsional element has special advantages. Warping restriction can be avoided, and the flapping and lead-lag stiffnesses can be tuned independently from each other. In addition the relatively high flapping stiffness of the torsional element reduces the static sag of the non-rotating rotor. Therefore no blade stop is needed.

Besides the described geometric reasons the special material properties of fiber composites are responsible for this low stiffness, as they extremely depend on the fiber orientation. For isotropic materials like metals the shear modulus G is directly coupled to the Young's modulus E via the Poisson's ratio v according to the formula: $G = E / [2 (1 + v)]$. This means that the shear modulus normally is about 2.6 times lower than the Young's modulus. For fiber composites this formula is no longer valid. Figure 7 shows the situation for E-Glass. The Young's modulus reaches its peak value of about 43000 Mpa (N/mm²) for the fiber orientation in 0° direction, whereas the shear modulus has its minimum of about 5000 Mpa there. For isotropic laminates the corresponding shear modulus would be about 16000 Mpa. The low shear modulus of the unidirectional laminate therefore provides an important share of the low torsional stiffness. The shear modulus reaches its peak at the ±45° fiber orientation (with a simultaneously low Young's modulus). As such ±45° laminates have the maximum shear and torsional stiffnesses and strengths, they are used to transfer torsional moments and transverse forces.

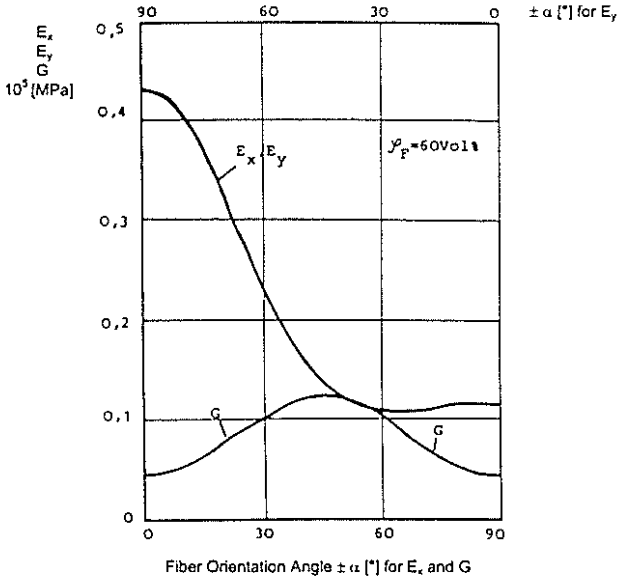

Figure 7: Young's and Shear Modulus in Dependence of the Fiber Orientation for Balanced Laminates (± Angles) and 60% Fiber Volume Content

The control cuff transfers the pitch angles to the blade. It is integral with the blade skin, therefore there is no joint in the skin at about 1.2 m radius. At this station the cuff is connected to the flexbeam via double C-profiles. Even if these profiles failed, the transfer of the pitch angles would be guaranteed via formlocking of the cruciform shape of the flexbeam. The ±45° GFRP sandwich skin gives a high torsional and low flapping stiffness. Unidirectional carbon fiber tapes at the leading and trailing edge of the cuff cause a high lead-lag stiffness. This generates high lead-lag forces and shear movements in the elastomeric dampers, so that they can provide sufficient damping. For each blade two dampers are attached at the top and at the bottom of the inboard end of the control cuff.

The total mass of the blade is almost 40 kg including about 7.5 kg of additional masses for the tuning of frequencies and the reduction mainly of the lead-lag bending moments.

These tuning masses are locally built in at several radius stations. Apart from the blade tip mass, they are enclosed by thermoplastic casings. A lot of care was taken over a fail safe fixation of these masses in the blade structure, as they locally generate high additional centrifugal forces. Each of two separate load paths can completely transfer the loads. Besides large-sized bonding areas being the first load path the masses are completely surrounded by blade structure, lugs, C-profiles etc., so that the centrifugal forces can also totally be carried via form-locking, even if the bonding had failed.

Main emphasis was laid on an excellent fail safe behaviour not only of the tuning masses but also of the complete rotor blade. The following table summarizes some of its characteristic features.

Table 2: Characteristic Fail Safe Design Features of the EC135 Main Rotor Blade

1. Flexbeam
   - Complete spar including flexbeam manufactured in one shot
   - 2 'double lugs' at the blade attachment

2. Control Cuff
   - Integral with blade skin
   - Double shear bonding of control cuff halfs
   - Form-locking design and double shear bonding of the connection to the pitch lever

3. Connection Control Cuff and Flexbeam (R = 1172 mm)
   - 2 load paths: a) large bonding areas
     b) form-locking design

4. Tuning Masses
   - 2 load paths: a) large bonding areas
     b) masses completely enclosed by supporting structures

3. CERTIFICATION REQUIREMENTS AND SUBSTANTIATION PRINCIPLES

As already mentioned the EC135 has been certified according to Joint Aviation Requirements JAR27 'Small Rotorcraft'. However, the certification of the rotor blade as well as of all other fiber composite parts had to be performed according to the 'Special Condition for Primary Structures Designed with Composite Material' of the LBA containing increased safety demands. This special condition adresses subjects like

- demonstration of ultimate load* capacity including consideration of manufacturing and impact damages
- fatigue evaluation for parts suitable or unsuitable for damage tolerance method and the related inspection procedures
- investigation of growth rate of damages that may occur from fatigue, corrosion, intrinsic and manufacturing defects or damages from discrete sources under repeated loads expected in service
- residual strength requirements
- consideration of the effects of material variability and environmental conditions like hot/wet strength degradation etc.
- substantiation of bonded joints

*The limit load which may occur once during the helicopter life must be proved with the safety factor 1.5. This increased load is called ultimate load.

Figure 8 shows possible certification methods. Because of the high service lifes due to the test results, the Flaw Tolerant Safe Life Evaluation was selected taking into account the additional safety requirements of the 'Special Condition'.

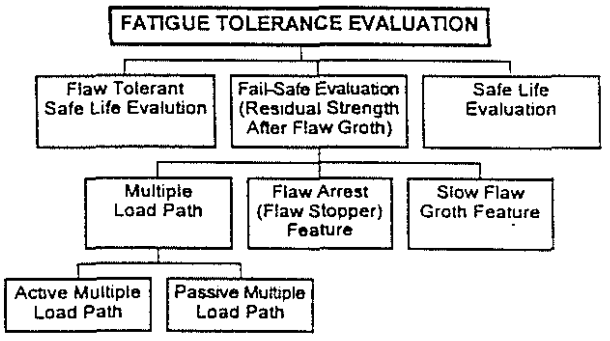

Figure 8: Possible Certification Concepts

The life of each rotor part was calculated by using a safe fatigue strength working curve (S/N-curve) derived from the component tests. The S/N-curve expressed in amplitude values is represented by the following relation:

$$S_A = S_{A\infty} + \frac{S_{A,ult} - S_{A\infty}}{\exp\left[\left(\frac{\log(N)}{\alpha}\right)^{\beta}\right]}$$

where $S_{A\infty}$ is the endurance limit, $S_{A,ult}$ the ultimate value, N the number of cycles and α, β are the shape parameters for the adjustment of the curve.

The flight tests yielded the necessary load spectra. A complete spectrum contains the working loads (High-Frequency-Spectrum) and the GAG loads (Ground-Air-Ground-Spectrum). The damage ratios and the resulting lifes of the structures were calculated according to Miner's linear damage accumulation hypothesis.

4. MATERIAL PROPERTIES OF THE FIBER COMPOSITES

The material stiffness and strength properties of the fiber composite materials were measured at ECD itself with the help of standardized coupon tests. The basic unidirectional stiffnesses and strengths were determined by long and short beam coupon specimens.

For the static strength substantiation interlaminar failure had to be avoided up to limit load. Up to ultimate load, however, no fiber failure was allowed. The strength degradations due to high temperature and moisture had also to be taken into account. For the fatigue strength substantiation room temperature conditions could be used. For the residual strength test with limit load after fatigue test the hot/wet degradation had to be considered again. As the blade is a fail safe structure, B-values could be taken for the substantiation.

Table 3 shows the tested material specimen types, the hot/wet conditions for the EC135 certification and the proceeding for the use of the allowables agreed with the certification authorities.

Table 3: Material Properties and Environmental Conditions

1. Material stiffness and strength properties determined by coupon tests:
   a) bending specimens (long beam type)
   b) shear specimens (short beam type)
2. Environmental conditions
   a) 75°C and 85% relative humidity (hot/wet conditions)
   b) room temperature conditions for fatigue strength substantiation
3. Allowables for material strength
   a) Ultimate load and residual strength
      - hot/wet conditions
      - $\sigma_{\perp}$ decisive (fiber crack)
      - No interlaminar failure (τ_{ILS}) allowed up to limit load
   b) Flight loads
      - room temperature conditions
      - B-values for substantiation of blade as fail safe structure

5. STRENGTH SUBSTANTIATION

5.1 Design of the Blade

At the beginning of the blade design the desirable natural frequencies of the blade were specified and the stiffness distributions were defined versus the blade radius in flapping and lead-lag direction. The various natural frequencies of the blade had to be separated from those of the rotor speed and its multiples as well as from the fuselage frequencies. Figure 9 shows the first four natural frequencies in flapping direction with the corresponding blade movements. (Each is normalized to 1 m blade tip displacement.) Analogously to the flapping direction the different lead-lag and torsion modes had also to be taken into account.

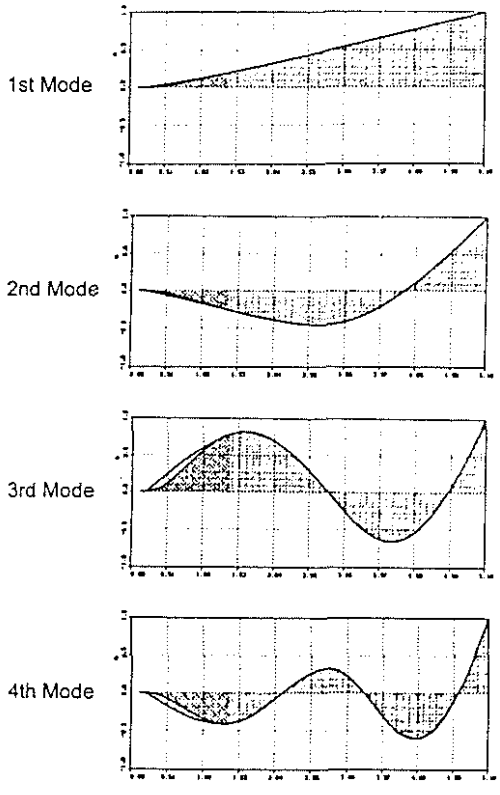

Figure 9: The First Four Bending Modes for the Rotor Blade in Flapping Direction; Blade Displacements versus the Radius

For the blade design, the cross section characteristics were calculated at various radius stations with the help of a two-dimensional finite element (FE) program. This ECD own code computes the six different stiffnesses corresponding to the forces and moments in the three coordinate directions. Additionally it also calculates the normal and shear stress distributions for any load combination. Figure 10 shows a typical FE modelization of the airfoil section.

Figure 10: FE Cross Section Modelization of the Airfoil Section

This FE analysis yields good results. However, it assumes that the cross section remains constant over a greater length. To determine additional stresses e.g. because of strong cross section variations, therefore a three-dimensional FE analysis needing a lot more effort was additionally performed (Fig. 11).

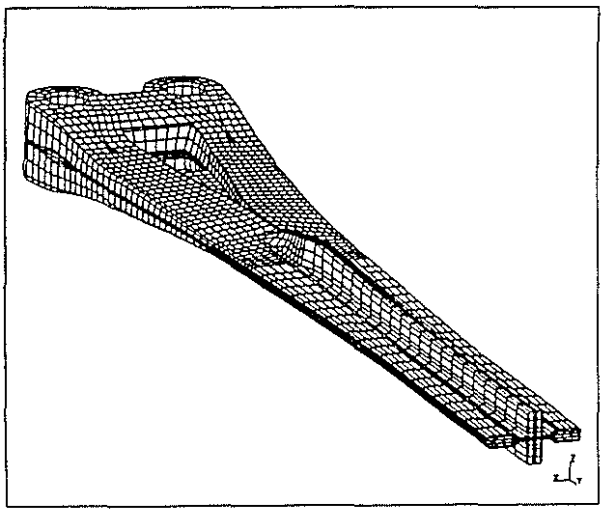

Figure 11: 3-Dimensional FE Model of the Prototype Flexbeam

5.3. Special Fracture Mechanics Investigations

Besides the centrifugal force the blade sections are mainly loaded either by torsion and/or bending. The failure modes of the blade were established with the help of structural dynamic tests. Delaminations due to torsional and bending stresses were studied by means of coupons and structural parts. In Figure 12 the three delamination modes are shown. The delamination mode I was eliminated by design whenever possible. Basic equations for bonded and tapered joints were derived for mode II and III. The relation between the transferrable stress σ_{II} and the peak shear stress τ_{max} was analysed by means of the classical 'shear-lag' theory and by fracture mechanics. For bonded joints the fracture mechanic property G_C is proportional to the thickness of the adhesive and to the square of the peak shear stress, devided by the shear modulus of the adhesive. G_C is the strain energy release rate.

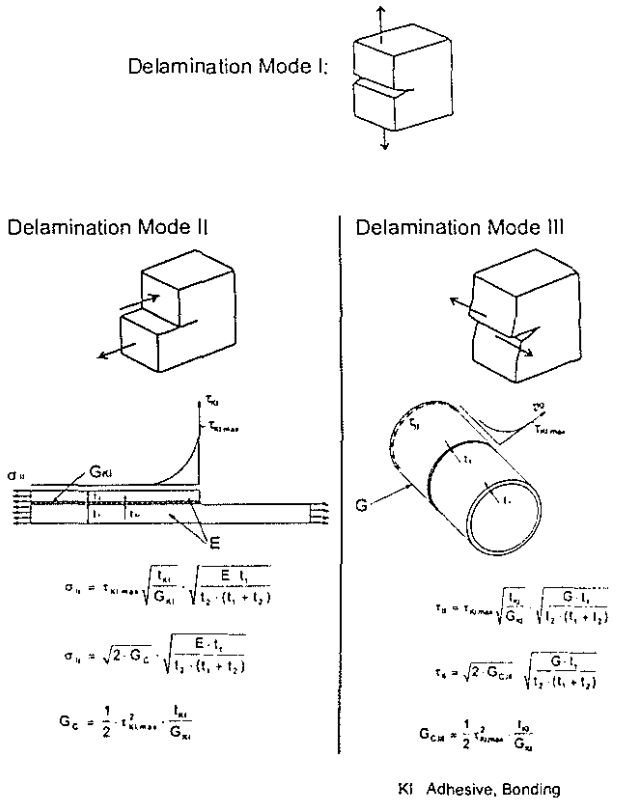

Figure 12: Delamination Modes of Overlaps and Joints and Relevant Delamination Formulas for Mode II and III

For the analysis of delamination initiation and propagation due to dynamic loads, tension test specimens with inner and outer fiber interruption were used. The damage tolerance behaviour was established for E-Glass/913 unidirectional prepregs used for the flexbeam of the EC135. The 'Transverse Crack Tensile' (TCT) test specimen with inner fiber interruption corresponds to the delamination mode II, whereas the specimen with outer fiber interruption takes the influence of mode I on mode II into consideration. The delamination stress σ_o for the stress ratio R=0 (swelling load) versus load cycles is shown in Figure 13. Because of the influence of mode I, the specimens with outer fiber interruption have a reduced strength with regard to delamination begin and a faster delamination propagation da/dN.

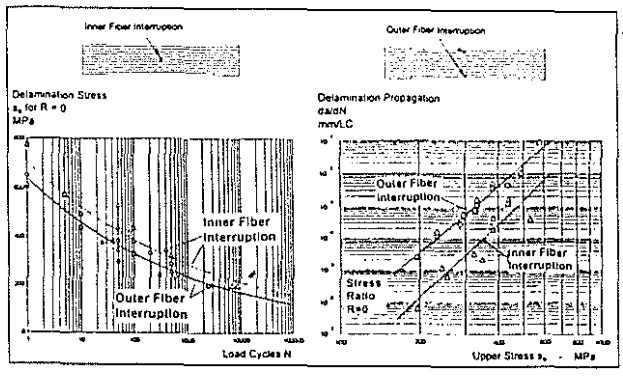

Figure 13: Basic Delamination Behaviour of the Unidirectional Laminate E-Glass/913 Prepreg Subject to Dynamic Tension Load

The strain energy release rate was calculated for different failure modes with the help of finite element models. The calculations were performed for the tapered root attachment area and the torsional cruciform section of the flexbeam. In addition, the delamination propagation was measured for a real torsional

element of the flexbeam subject to centrifugal force and torsional moments (see Fig. 14). The comparison with the basic coupon test data showed a good coincidence.

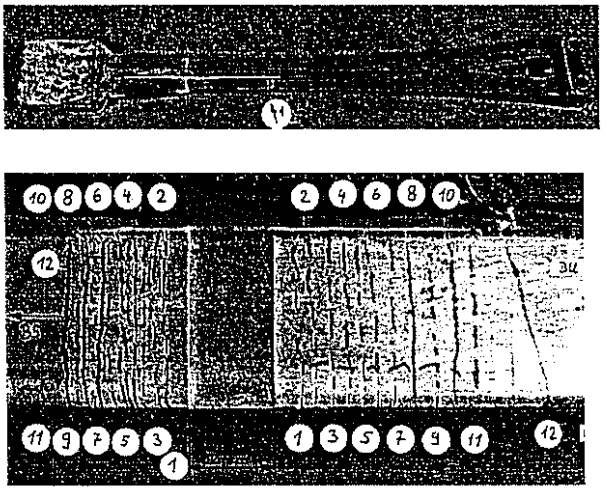

Figure 14: Artificial Damage in the Torsional Element of the Flexbeam; Delamination Propagation due to Torsional Loads and Constant Centrifugal Force

6. MANUFACTURING OF THE ROTOR BLADE

The complete spar of the blade including flexbeam is premanufactured in one shot. It includes the unidirectional layers of the blade, the shear web laminates in the flexbeam and most of the tuning masses. Figure 15 shows how the unidirectional layers of the spar are put in one mould half.

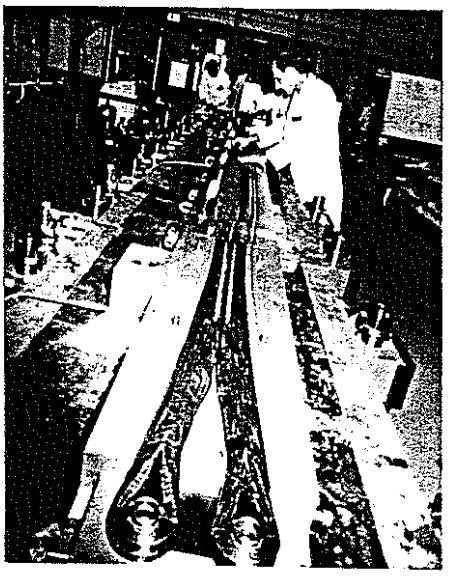

Figure 15: Manufacturing of the Blade Spar Including Flexbeam

As the flexbeam is the highest loaded part of the blade, the fibers must be tightened mainly in the critical lug area (in the foreground) to prevent waves in the laminate. After the strong blade attachment the cross section area is halved on a relatively short length towards the 'flapping hinge'. Therefore many layers have to be tapered. Because of the high strains in this region only small taper steps of 0.2 and 0.3 mm are allowed, which furthermore have to be in the inner part of the structure near the neutral axis. These measures prevent high shear stress peaks and the peeling off of layers. In addition the optimum fiber volume content has to be kept in small limits to prevent the shifting of fibers at overfilling or air inclusions at underfilling. Therefore for each spar more than 10 material coupon specimens are examined to determine the ply thickness and the fiber volume content of the prepreg material exactly. Depending on these results a special calculation program computes the necessary number of layers and the length of the tapered layers for each spar. This process is necessary to guarantee an optimum laminate quality and strength especially for the flexbeam.

7. QUALITY ASSURANCE

As it was done during the design phase, a computer tomography (CT) examination has been performed for each blade at the beginning of the serial production.

Originally CT was developed for the medical field. To create a cross section image, an X-ray beam rotates around the object in a complete circle. From several projection directions attenuation profiles of the beam are measured. With these data a computer calculates the image of the cross section slice having the thickness of the X-ray beam of about 1.5 mm. During the rotor blade examination cross section images are produced at various radius stations. When these stations are close together, e.g. in the lug area, vertical and horizontal cuts in radial direction can also be computed.

CT is a very effective non-destructive testing (NDT) method to check the quality of fiber composite parts. Damages or defects like cracks or waves in the laminate of at least 0.2 mm size can be detected. By the determination of special CT numbers the local material density can be established. Thus e.g. it can be checked if dark spots in a cross section consist of resin or critical air inclusions. With the help of CT, the manufacturing quality of the EC135 blade could be improved remarkably (Fig. 16).

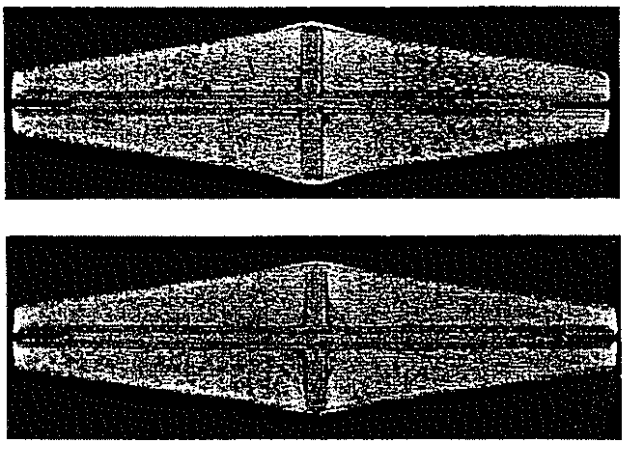

Figure 16: CT Image of a Flexbeam Cross Section;
Above Prototype Blade with Resin and Air Inclusions,
Below Serial Quality with Uncritical Resin Inclusions

A test specification for the EC135 main rotor blade describes in detail, in which area which kind of damages are allowed. If a new type of damage occurs seeming to be eventually critical, a component test is performed. This test has to prove, if the damage affects the life of the structure. When it does, this damage is not accepted for the serial blade quality.

8. STRUCTURAL TESTS

8.1 Rotor Hub and Shaft

Several rotor hub specimens including shafts were subjected to the simulated centrifugal and transverse forces and moments of all four blades. The resultant dynamic forces were introduced by the four slightly sloping hydraulic cylinders in Fig. 17 at the fictious flapping hinge offset. (Rotor hub and shaft are vertically mounted at the left side of the photo between the hydraulic cylinders.) The cylinders produced lead-lag moments and a circulating shaft bending moment. Figure 18 shows the final crack of the first prototype version.

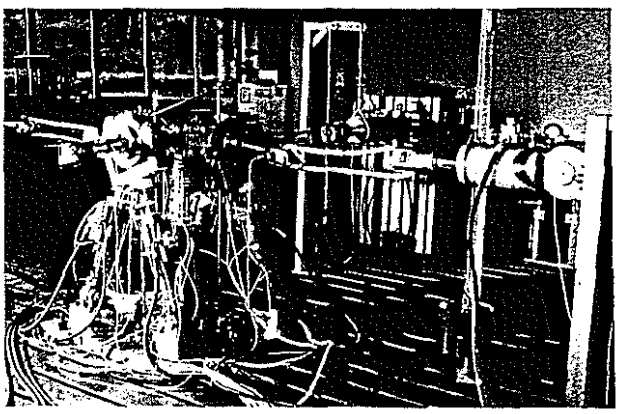

Figure 17: Rotor Hub and Shaft in the Bending Test

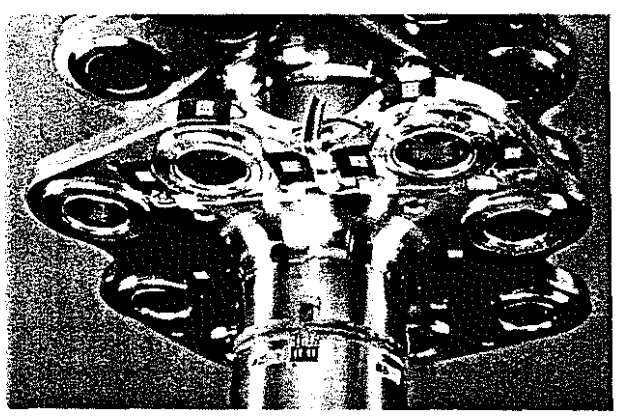

Figure 18: Crack in the Transition Area between Shaft and Hub of the Prototype Version

Due to geometry improvements during the development phase mainly in the transition area between shaft and hub the S/N-curves could be raised by almost 20%. This led to an infinite life at the actual maximum take-off weight.

8.2 Rotor Blade

It is not possible to test a complete blade realistically at all possible load combinations in a testing machine. Therefore the blade was subdivided into several components each of them being tested under its critical load conditions. For each test type several specimens with intrinsic, manufacturing and impact damages were tested at different load levels. The impact energy for flexbeam and control cuff was 25 J. This means a 2.5 kg impact mass falling down from 1 m height.

For the static ultimate load tests the influence of high temperature and moisture had to be taken into account according to the 'Special Condition'. The strength degradation was determined by coupon tests, s. chapt. 4. The static component tests were then performed at room temperature with loads increased by the hot/wet degradation factors. The maximum loads were simultaneously applied to cover the worst case possible.

After the fatigue tests residual strength tests had to be performed. Limit load capacity was proven there, also including load amplification factors to simulate hot/wet conditions.

Table 4 summarizes the process for the component tests taking into account the requirements of the 'Special Condition'. These tests were the basis for the life calculations.

Table 4: Process for the (Sub-)Component Tests

1. Component specimens
   - Specimens with intrinsic, manufacturing and impact damages

2. Tests
   - Separate component tests for critical areas
   - Constant amplitude tests at different load levels
   - Test monitoring
   - Documentation of: Type of damage
     Damage begin
     Size
     Location
     Growth rate

3. Residual strength test with predamaged specimens after fatigue test
   - Proof of Limit Load capacity
   - Load amplification factor to simulate hot/wet conditions

Among others following (sub)component tests were performed:

- Flexbeam:
  a) Inner blade root section:
     centrifugal force
     flapping and lead-lag moments
     transverse forces
     torsional moment due to bending
  b) Torsional element:
     centrifugal force
     torsional angles (pitch angles) and start/stop cycles (swelling centrifugal force) in between times
- Control Cuff:
  a) centrifugal force
     flapping and lead-lag moments
     transverse forces
  b) centrifugal force
     torsional moment
- Airfoil Section (proof of manufacturing quality; not relevant for certification):
  a) resonance bending (alternating dyn. bending)
  b) tension-torsion
- Tuning Masses:
  a) centrifugal force to test the bonding
  b) centrifugal force to test the form locking feature of the surrounding structure

Figure 19 shows a bending specimen of the flexbeam in its upper and lower test position. It is pretensioned by a centrifugal force of about 150 kN and simultaneously loaded by flapping and lead-lag moments (number a of the flexbeam tests from above). At the left side the blade attachment area is clamped in to a fork simulating the rotor hub. At the right side two hydraulic cylinders

introduce the maximum transverse forces and flapping and lead-lag moments simultaneously. This test mainly simulates the load conditions between blade attachment and 'flapping hinge'.

During the development phase the flexbeam was continuously improved and the S/N-curve concerning bending could be raised by about 20%.

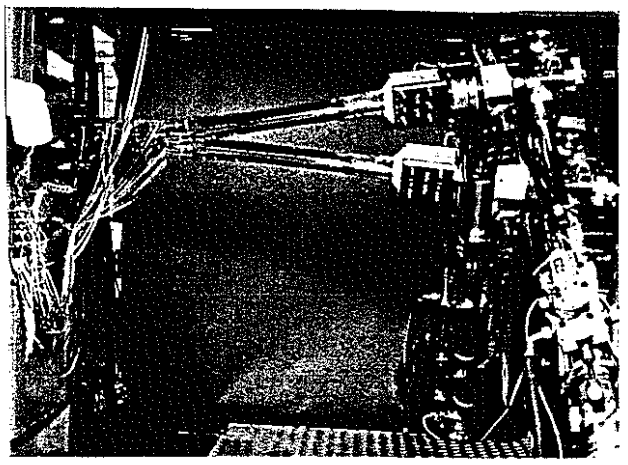

Figure 19: Flexbeam Specimen Loaded by Bending Moments and Centrifugal Force

The torsional capability of the flexbeam was proved in another test sequence. Figure 20 shows the specimen unloaded. The cuff is almost completely removed. At the right side the blade attachment area of the flexbeam is clamped. (To the left it is followed by the flat 'flapping hinge' and the torsional element with its slit cruciform cross section.) In Figure 21 the specimen is pretensioned by a centrifugal force of 150 kN and is twisted by 100°. This means a torsional angle of 2°/cm length of the torsional element. The specimen showed no failure, the test was only limited by the capacity of the testing machine. This test proved the outstanding qualities of the EC135 flexbeam.

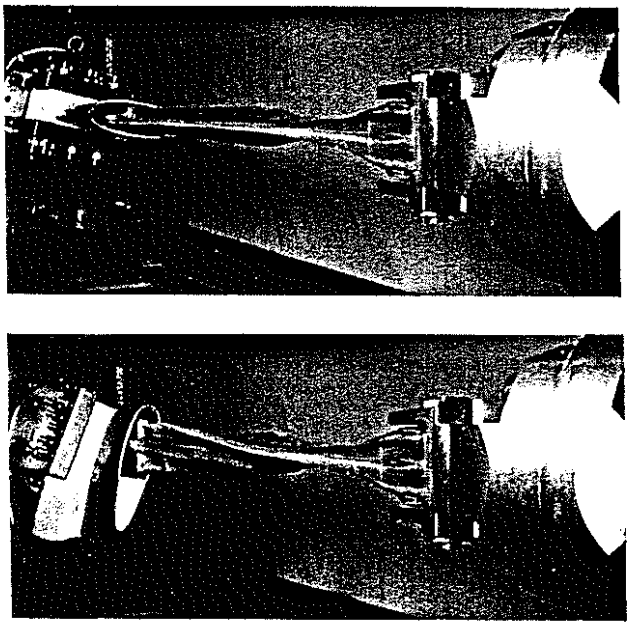

Figures 20 and 21: Above Flexbeam Unloaded;
Below Flexbeam Loaded by Centrifugal Force and Twisted by 100 °

In Figure 22 the bending test for the control cuff is shown.

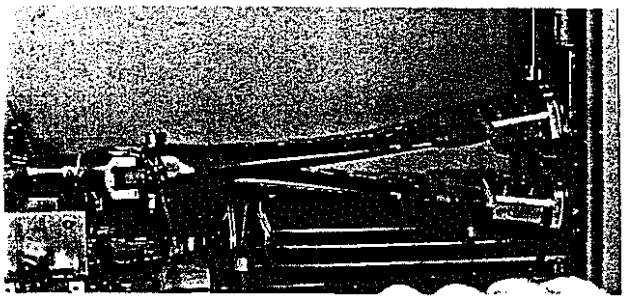

Figure 22: Control Cuff Specimen in the Bending Test

9. DAMAGE TOLERANCE BEHAVIOUR OF THE BLADE

In all tests the rotor blade showed an excellent fail safe behaviour. The 25 J impact damages had no influence on the life of the specimens. Occurring damages showed no or only very slow crack growth during the fatigue tests. Many of these tests were performed at such a high load level that the last load cycle was already the residual strength test demanded by the LBA.

The critical part of the blade concerning helicopter safety is the blade attachment area with the lugs. In no residual strength test after the bending test it was possible to crack a complete double lug. The horizontal shear web in the center plane stopped the crack to a great extent. Even if the blade lost some of its stiffness, the limit loads could still completely be transferred.

The blade attachment area can well be examined by visual inspection. Furthermore there are special uncritical damages, which occur early enough before the lug crack starting at the bore hole reaches the outer edge of the laminate and becomes visible. This damages are used as in time warnings and develop as follows. First the bonding between bearing laminate and unidirectional fibers fails almost completely during a long service period (s. Figure 23). Then the bearing laminate cracks vertically from the bolt to the outer edge. And then the lug crack moves towards the outside. However, this is not critical yet for flight safety. In service only the debonding of the outer part of the bearing laminate is allowed up to the step in the laminate. Then the blade has to be checked e.g. by computed tomography if already a lug crack has started.

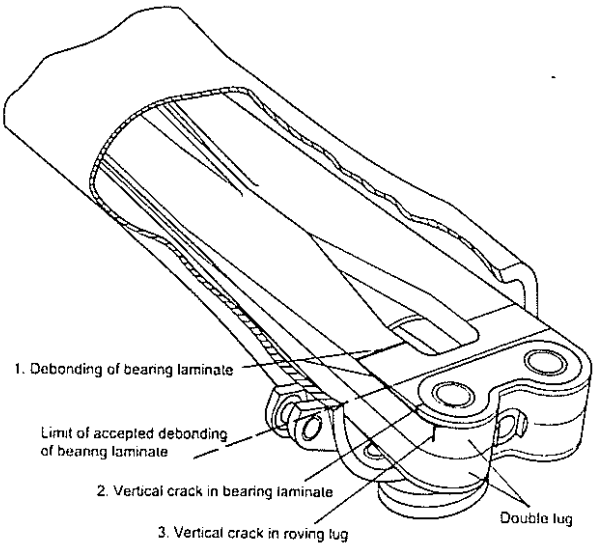

Figure 23: The Damage Behaviour of the Blade Attachment Area

10. SUMMARY

The EC135 is a twin-engined multi-mission light helicopter of the new generation. It has been designed to meet the latest airworthiness requirements as well as today's stringent operational demands. One of its outstanding features is the bearingless main rotor which integrates the best technology from a long rotor development line at ECD.

During the last decades the former helicopter division of MBB and now Eurocopter Deutschland has consequently developed the main rotor systems towards simplification, improved reliability, increased life, lower weight and reduced service and maintenance costs. It started with the hingeless rotor of the BO105 and continued to the bearingless rotor of the EC135. However, this became only possible by using the outstanding qualities of glass fiber composites with regard to strength and flexibility.

The certification tests proved the excellent fail safe and damage tolerance characteristics of the EC135 main rotor. Its design will be the basis for new rotor systems in the future. The first step has already been done in the company with the start of a new research program concerning advanced bearingless main rotors.

Orders of more than 120 EC135 in the relatively short time since its certification show that this helicopter with its innovative bearingless rotor system has been well accepted by customers worldwide.

11. REFERENCES

[1] S. Attlfellner,
'Eurocopter EC135 Qualification for the Market',
22nd European Rotorcraft Forum,
Brighton, UK., 17-19 September 1996

[2] H. Bansemir, R. Mueller,
'The EC135 - Applied Advanced Technology',
AHS, 53rd Annual Forum,
Virginia Beach, USA, 29 April - 1 May 1997

[3] H. Barnerssoi, A. v. Panajott, K. Pfeifer, R. Vorwerg,
'EC135 Structural Testing',
23rd European Rotorcraft Forum, Dresden, Germany,
16-18 November 1997

[4] D. Braun,
'Ground and Flight Tests of a Passive Isolation System for Helicopter Vibration Reduction',
8th European Rotorcraft Forum and Powered Lift Aircraft Forum,
Aix-en-Provence, France, August 1982

[5] D. Hamel, A. Humpert,
'Eurocopter EC135 Initial Flight Test Results',
20th European Rotorcraft Forum,
Amsterdam, the Netherlands, 4-7 October 1994

[6] H. Huber,
'Will Rotor Hubs Loose Their Bearings ?',
A Survey of Bearingless Main Rotor Development,
18th European Rotorcraft Forum,
Avignon, France, 15-18 September 1982

[7] H. Huber, C. Schick,
'MBB's BO108 Design and Development',
46th Annual Forum & Technology Display of the American Helicopter Society,
Sheraton Washington Hotel, Washington D.C.,
21-23 May 1990

[8] R. Oster,
'Computed Tomography as a Nondestructive Test Method for Fiber Main Rotor Blades in Development, Series and Maintenance',
23rd European Rotorcraft Forum, Dresden, Germany,
16-18 September 1997

[9] G. Seitz, G. Singer,
'Structural and Dynamic Tailoring of Hingeless/Bearingless Rotors',
9th European Rotorcraft Forum,
Stresa, Italy, 1983

[10] V. von Tein, C. Schick,
'BO108-Technology for New Light Twin Helicopters',
14th European Rotorcraft Forum,
Milano, Italy, September 1988

[11] M. Vialle, C.Avand,
'A New Generation of Fenestron = Fan-in-Fin Tail Rotor on EC135',
19th European Rotorcraft Forum, Cernobbio, Sept. 1993

[12] M. R. Wisnom,
'Delamination in Tapered Unidirectional Glass Fibre Epoxy at Static Tension Loading',
Proc. AIAA Structures,
Structural Dynamics and Materials Conference,
Baltimore, April 1991, pp. 1162 - 1172

[13] C. Zwicker,
'Configuration and Program Status of Eurocopter's EC135',
19th European Rotorcraft Forum, Cernobbio, Sept. 1993

[14] D. Schimke, B. Enenkl, E. Allramseder,
'MBB BO 108 Helicopter Ground and Flight Test Evaluation',
15th European Rotorcraft Forum,
Amsterdam, the Netherlands, 12-15 September 1989